

Preparation of Carbon-based Magnetic Solid Acid Catalyst from Various Carbon Sources and Characterization of its Catalytic Performance

Xueqin Li,^{a,b,c} Junyou Shi,^b Zhiwei Wang,^{a,c} Xixin Duan,^b Gaofeng Chen,^{a,c} Qian Guan,^{a,c} Xiangyu Li,^{b,*} and Tingzhou Lei^{c,d,*}

Four kinds of carbon-based magnetic solid acid catalysts (CBMSACs) were prepared from rice husk, wood chips, peanut shells, and corn straw. The structure was investigated *via* x-ray diffraction (XRD), Fourier transform infrared spectroscopy (FT-IR), elemental Analysis (EA), scanning/transmission electron microscope (SEM/TEM), and BET analyses. The catalysts were used to hydrolyze cellulose, and the hydrolysis efficiencies were determined. The catalysts were all comprised of a disordered carbon structure with random polycyclic aromatic hydrocarbons similar to graphite layers. This structure had a large number of -SO₃H groups and the alkyl side chain, which increased the electron cloud density of the carbon carrier, relative to the other catalysts; this was advantageous to the adhesion of the -SO₃H group to increase the activity of catalysts. The product also contained a large number of magnetic particles, making it easy to separate the catalysts from the reaction residue. The properties of the catalyst derived from corn straw as the carbon source appeared to be the best. Although it could be further recycled many times, the catalyst activity decreased due to the loss of -SO₃H groups. At the same time, the catalyst had a high specific surface area of 755 m²/g.

Keywords: Biomass; Carbon-based magnetic solid acid catalyst; Catalytic hydrolysis; Disordered carbon structure

Contact information: a: Energy Research Institute Co., Ltd., Henan Academy of Science, Zhengzhou, China, 450008; b: Wood Material Science and Engineering Key Laboratory, Beihua University, Jilin Province, Jilin, China, 132013; c: Key Biomass Energy Lab of Henan Province, Zhengzhou, China, 450008; d: Henan Academy of Science, Zhengzhou 450008, China;

* Corresponding author: lixiv@126.com; leitingzhou@163.com

INTRODUCTION

Biomass resources can be used to prepare carbon-based carriers containing numerous oxygen and hydrogen functional groups by the method of carbonization and sulfonation; such carriers can attack the β -1,4 glycosidic bonds to result in lower bond energy (Sathishkumar *et al.* 2012). These carbon-based materials of inherent hydrophobic graphite layer-like structure possess very high catalytic activity in the water phase (White *et al.* 2009), but the physical properties of carbon-based catalysts are similar to the properties of hydrolysis residue produced from hydrolysis of lignocellulosic biomass. Thus, the carriers are difficult to recover and reuse. However, at present, most of magnetic solid acid catalysts essentially use magnetic particles as a core (Ke *et al.* 2013), and most of the functional groups would be loaded on the surface of the magnetic particle that has been modified (Chang *et al.* 2002). This decreases the stability and catalytic activity of the

catalyst. Thus, using biomass as carbon materials is beneficial, as its simple surface activation treatment would prepare the carbon-based magnetic solid acid catalysts (CBMSAC) (Zhang *et al.* 2015). The simplicity of this method makes it a hot research topic and cutting-edge technology in the catalyst field. Corn straw has been used as raw material to optimize the condition of biomass-based solid acid catalyst preparations (Zhang *et al.* 2015). However, biomass is comprised of many oxygen-containing functional groups that would fall off in the form of water during the carbonization process, which will reduce the carbon carrier yield (Keiluweit *et al.* 2010). The catalytic activity of catalysts is also influenced by many factors (*e.g.*, size of magnetic aromatic lamella in catalyst, neat degree of stability, density of active group, kinds of auxiliary group, and so on) (Yu *et al.* 2013). In addition, using different raw materials as carbon sources may lead to structural variation of the catalyst. Thus, it is necessary to study the CBMSAC prepared with different carbon sources. China's huge biomass resources include high contents of corn straw (CS), wood chips (WC), rice husk (RH), and peanut shells (PS). These raw materials have been generally burned as fuel, which is a great waste. The quantitative chemical analysis (Table 1) on four kinds of materials has shown that each has advantages in establishing a resource-efficient economy.

Therefore, this study used four kinds of biomass materials to prepare CBMSACs. Cellulose was used as a model compound, and the total reducing sugar yield was used as an indicator to characterize the catalytic activity of these catalysts. The X-ray diffraction (XRD), Fourier transform infrared spectroscopy (FT-IR), elemental analysis (EA), scanning/transmission electron microscope (SEM/TEM), and BET analysis were employed to characterize the surface structure and functional groups on the prepared catalysts. Compared with the conventional carbon solid acid catalyst (Chu *et al.* 2011), the characteristics of CBMSACs were similar with the cellulose hydrolysis residue. However, due to the presence of the magnetic particle property, the catalyst was easy to be separated from the hydrolysis residue after the catalytic hydrolysis of cellulose. Therefore, CBMSACs have very high catalytic activity, easy recovery, and a high utilization rate. The interaction between the CBMSAC and cellulose particles is illustrated in Fig. 1.

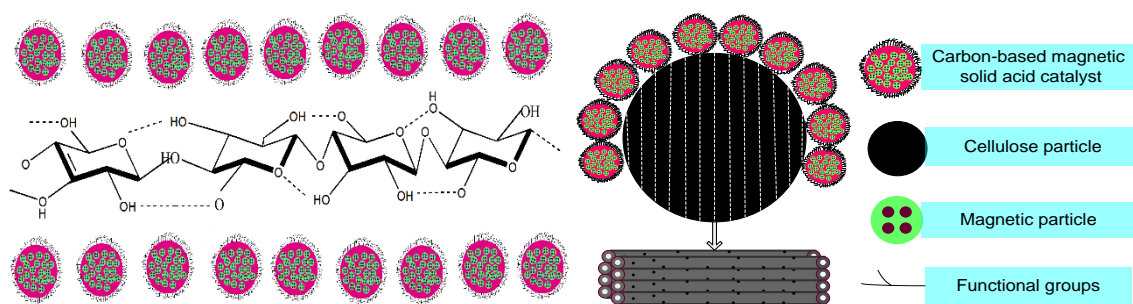


Fig. 1. Interaction between magnetic catalyst and cellulose particles

EXPERIMENTAL

Materials

Preparation of carbon-based magnetic solid catalyst

Magnetic Fe_3O_4 particles and the carbon-based precursor were mixed according to a quantity ratio of 1:2 and soaked in 1 mol/L H_2SO_4 solution for 24 h.

The mixture was then suction filtered, and the retained solids were dried. The dried product was calcined in a muffle furnace at 500 °C for 3 h to obtain the CBMSAC. The preparation process is shown in Fig. 2.

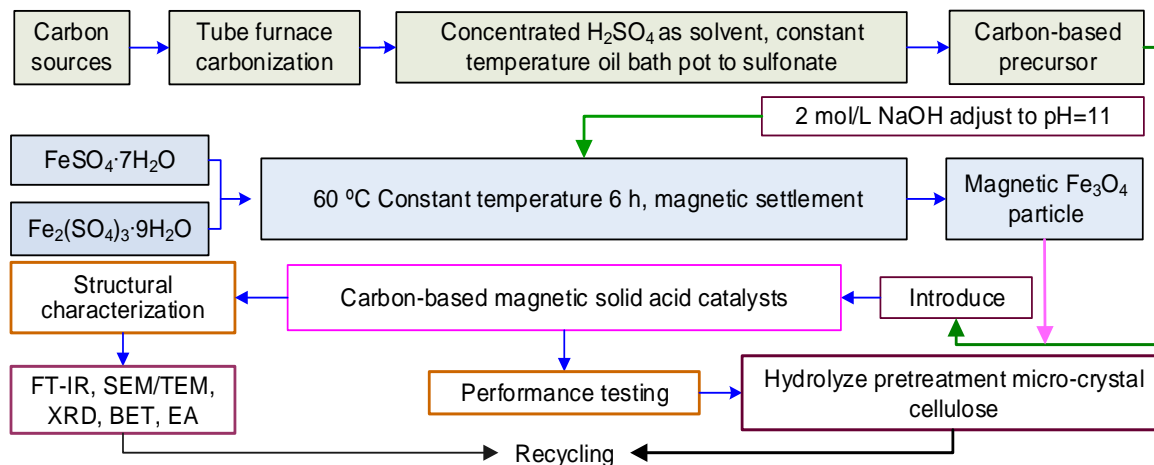


Fig. 2. Process diagram for carbon-based magnetic solid acid catalyst preparation

Methods

Structural characterization

A FT-IR (EQUINOX55, Bruker, Berlin, Germany) was used to analyze the functional groups of CBMSACs. A SEM (Tcnai G² 20, FEI, Hong Kong, China) and TEM (Quanta 200, FEI, Hong Kong, China) analysis was employed to observe the surface morphology of CBMSACs. An XRD device (X'pert PRO MPO, Almelo, Netherlands) was used to analyze the crystal structure of CBMSACs. The BET analysis (V-sorb 2800, Gold APP Instrument Corporation, China) was used to determine the specific surface area, and EA (EA300-Single, EURO, Italy) provided the elemental composition of CBMSACs.

RESULTS AND DISCUSSION

Quantitative Compositional Analysis of Various Carbon Sources

Table 1 shows that the content of cellulose in WC, CS, and PS was higher than in RH; The ash content was high in the RH and PS and it was relatively lower in the CS and WS. If CS and PS were used as raw materials for the combustion, it will cause a certain influence to the life of the combustion equipment (Nunes *et al.* 2016). In general, the less the volatile content, the more fixed carbon content (Chen *et al.* 2012).

Table 1 shows that the content of fixed carbon was higher in CS compared to the other sources. This result indicates the CS is an important raw material for the synthesis of biomass chemicals.

Table 1. Compositional Analysis of Different Carbon Sources

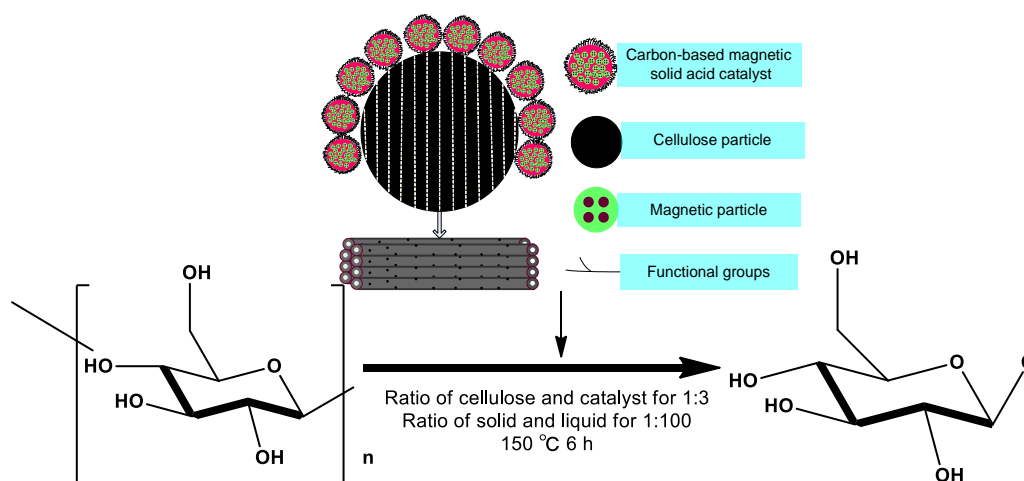
| Sample | Water (%) | Ash (%) | Volatile (%) | Fixed Carbon (%) | Cellulose (%) | Lignin (%) | Hemi-cellulose (%) |
|--------|-----------|---------|--------------|------------------|---------------|------------|--------------------|
| WC | 6.2 | 1.4 | 68.0 | 24.5 | 42.3 | 16.2 | 27.7 |
| CS | 8.3 | 5.0 | 50.7 | 27.1 | 42.7 | 17.5 | 23.6 |
| RH | 17.3 | 16.1 | 0.6 | 75.1 | 37.0 | 13.6 | 22.7 |
| PS | 9.3 | 15.1 | 60.4 | 15.5 | 43.0 | 26.9 | 16.9 |

Performance of Catalyst in Cellulose Hydrolysis

The conversion of cellulose was evaluated using the prepared catalyst (Du *et al.* 2004). A mixture of cellulose and CBMSACs in a ratio of 1:3 was first added to 100 mL of distilled water and allowed to react for 6 h at 150 °C. After the reaction followed by centrifugal separation, the reducing sugar yield was determined in the hydrolysate by the method of phenol-sulfuric acid, and the catalyst was isolated and recycled. The hydrolysis reaction mechanism is shown in Fig. 3. Table 2 and Fig. 4 show that the reducing sugar yields obtained from the catalytic hydrolysis of cellulose by PS- and CS-BMSACs were higher. This showed that the performance of these two kinds of catalyst was better; the performance of CS-BMSAC (58.8%) appeared to be the best, and compared to the traditional catalysts (Yu *et al.* 2013), there was an approximately 5% increase of catalytic efficiency.

Table 2. Various Carbon-based Magnetic Solid Acids Catalyzed Cellulose Hydrolysis-performance Comparison

| Catalyst-Type | Reaction Condition | Reduced Sugar Yield (%) |
|---------------|--|-------------------------|
| RH-BMSAC | Carbonization at 549 °C, 13 h Sulfonation at 121 °C, 6 h Calcination at 500 °C Calcination at 3 h | 38.4 ± 3 |
| WC-BMSAC | | 47.6 ± 4 |
| PS-BMSAC | | 55.9 ± 2 |
| CS-BMSAC | | 58.8 ± 3 |

**Fig. 3.** Mechanism of hydrolysis of Cellulose

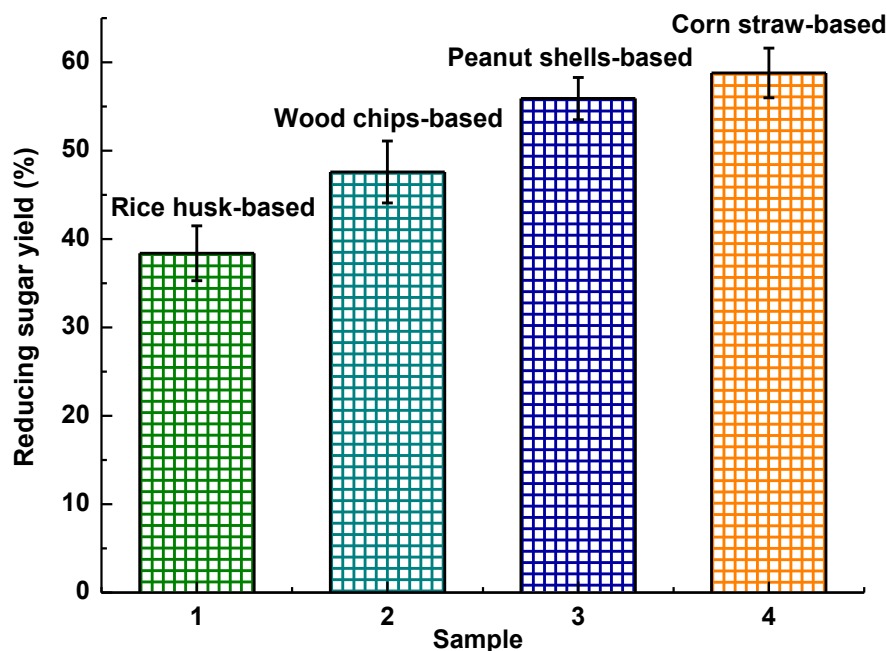
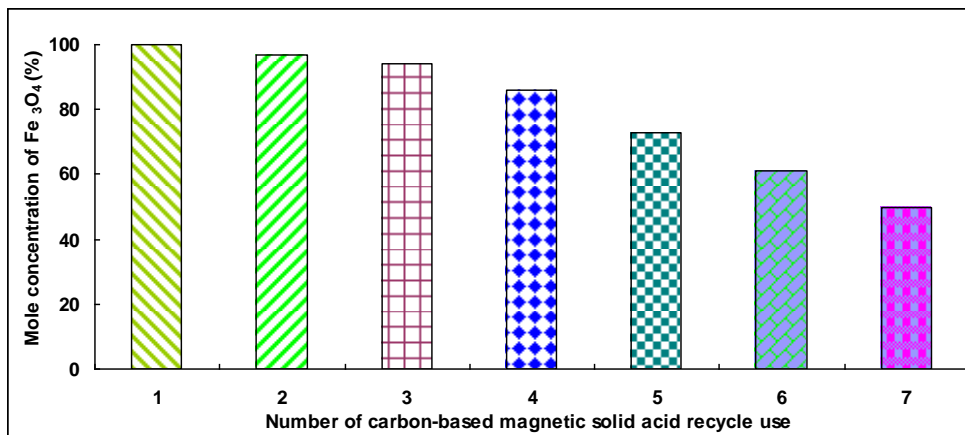


Fig. 4. Comparison of reducing sugar yields

Recovery and Regeneration of Catalyst

The catalysis of cellulose hydrolysis, which used the four kinds of CBMSACs as catalysts, showed that the performance of CS-BMSAC was enhanced. Therefore, to investigate the recovery and regeneration of catalysts, CS-BMSAC was recycled in a series of catalytic cellulose hydrolysis reactions.

Figure 5 shows that the reducing sugar yield gradually decreased with the increase of catalyst reuse times and that the mole concentration of magnetic Fe_3O_4 particles also decreased with the increase of catalyst reuse times. In other words, the catalytic performance gradually decreased with the increase of catalyst reuse times. Analyzing the hydrolysis process of cellulose showed that the catalyst activity decreased because of the loss of a portion of the $-\text{SO}_3\text{H}$ groups. Therefore, the activity of catalysts was re-achieved via a re-sulfonation method.



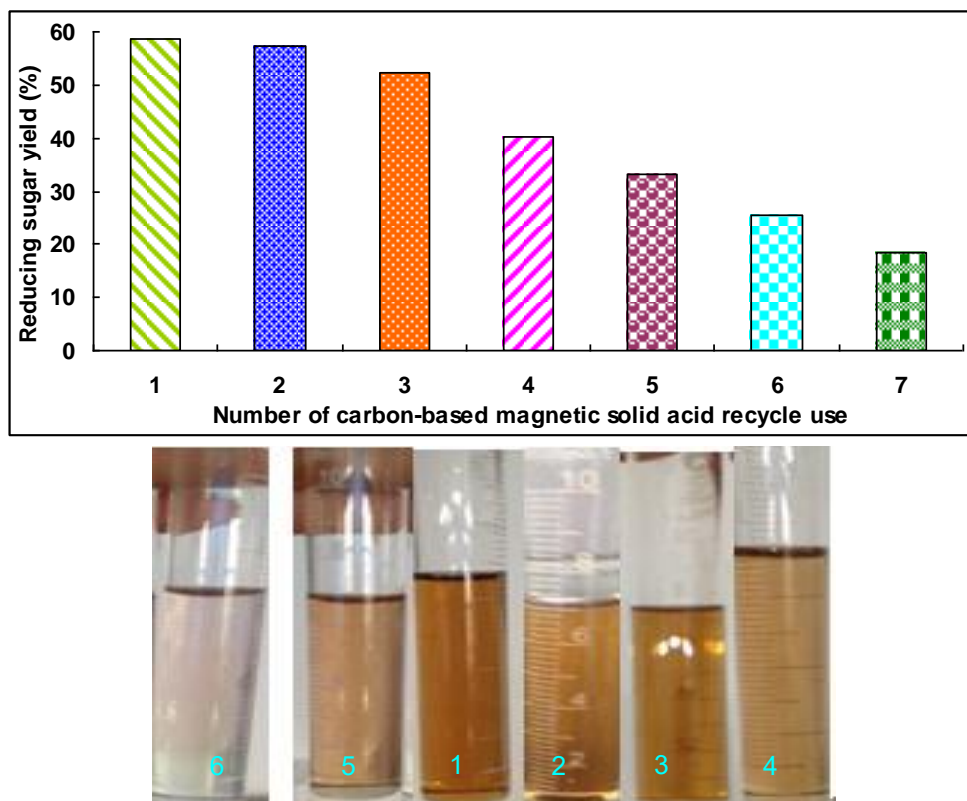


Fig. 5. Repeated use of catalyst

Catalyst Characterization

The research of Wu *et al.* (2009) shows that the change of the carbon element was not obvious and the content of S element showed obvious change after biomass sources were calcined.

The content of C element in the four kinds of catalysts was between 41% and 44%, as shown in Table 3. However, in the CS- and PS-BMSACs the content of S element was higher; this showed that the surface of catalysts that used CS and PS as raw material for preparation were combined with a large number of $-SO_3H$ groups, which likely played a role in increasing the activity of catalysts.

Table 3. Elemental Analysis of Various Catalysts

| Cat-type | C (%) | H (%) | N (%) | S (%) | O (%) | Molecular Formula |
|----------|-------|-------|-------|-------|-------|-------------------------------------|
| CS-BMSAC | 43.2 | 4.4 | 1.1 | 4.6 | 14.8 | $CH_{0.4}N_{0.005}S_{0.2}O_{0.01}$ |
| RH-BMSAC | 41.6 | 3.0 | 0.4 | 1.5 | 0.5 | $CH_{3.3}N_{0.7}S_{0.04}O_{0.1}$ |
| WC-BMSAC | 42.8 | 3.0 | 0.4 | 2.0 | 0.5 | $CH_{0.3}N_{0.002}S_{0.05}O_{0.01}$ |
| PS-BMSAC | 44.6 | 4.1 | 1.2 | 4.4 | 0.5 | $CH_{0.3}N_{0.02}S_{0.2}O_{0.01}$ |

FT-IR Analysis

Figure 6 reveals the infrared spectra of four kinds of CBMSACs. Based on previous literature (Zhou *et al.* 2001; Berry *et al.* 2003; Sinirlioglu *et al.* 2014), the absorption peak

at 598 cm^{-1} belongs to an -OH bending vibration, and the peak at 1025 cm^{-1} represents the symmetric and anti-symmetric of stretching vibrations of the O=S=O bond in -SO₃H groups. This peak confirmed that many -SO₃H groups were introduced into the four kinds of catalysts. The peaks at 1500 cm^{-1} to 1675 cm^{-1} belong to the stretching vibration of the C-C bond. The absorption peak at 1600 cm^{-1} to 1900 cm^{-1} represents the stretching vibration of a C-O bond, and the absorption peak at 2375 cm^{-1} to 2500 cm^{-1} belongs to the stretching vibration of an S-H bond. In addition, the absorption peak of 1380 cm^{-1} belonged to the stretching vibration of the -CH₃ group that came from the carbon source itself. As can be seen in Fig. 6, the CS-BMSAC peaks at 2375 cm^{-1} to 2500 cm^{-1} and 1380 cm^{-1} were noticeable, which showed that the CS-BMSAC possessed a large number of -SO₃H groups. This characteristic was responsible for its stability and catalytic performance.

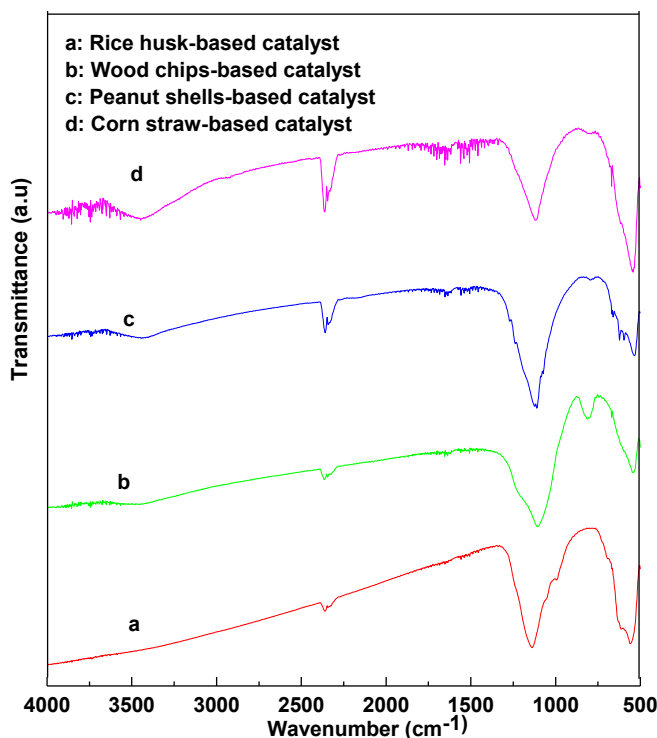


Fig. 6. Infrared spectra of different catalysts

XRD Analysis

The XRD spectra of the four kinds of BMSACs are shown in Fig. 7. All of the BMSACs exhibited a diffraction maximum in the range $2\theta = 33^\circ$ to 36° . The peak intensity gradually increased from Figs. 7a to 7c, which showed that the BMSACs were composed of a disordered carbon structure that was formed by crystalline aromatic hydrocarbons similar to graphite layers in a random ways. In Figs. 7a and 7d, the diffraction peak was considerably stronger and moved in a high angle direction. This demonstrated that the polymerization degrees of CS- and PS-BMSACs were higher and their structure was more stable.

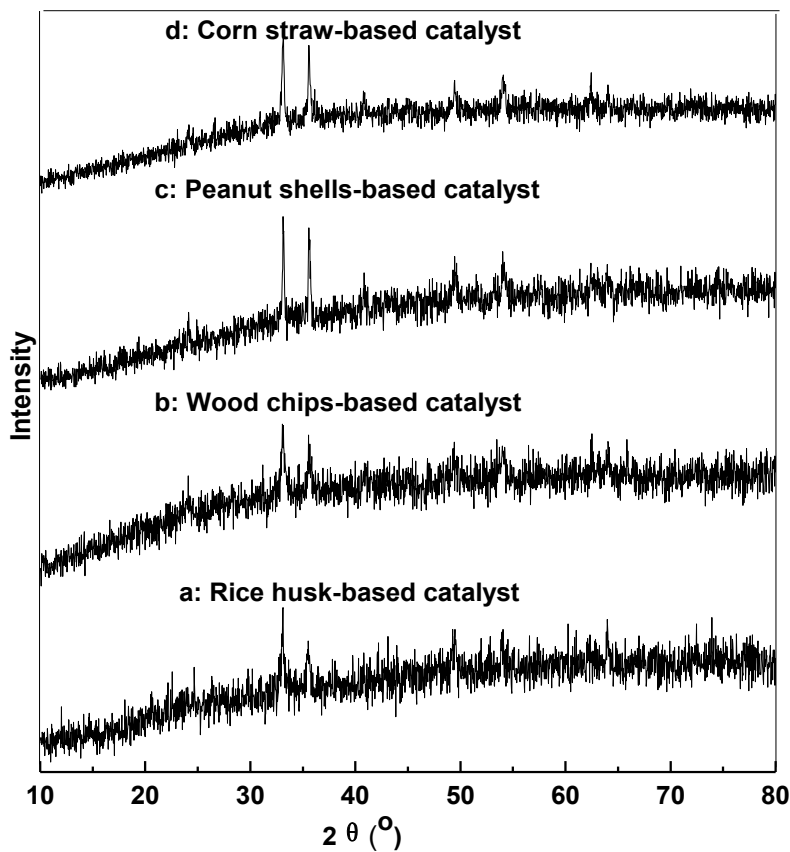


Fig. 7. XRD patterns of different catalysts

TEM Analysis

Figure 8 displays the TEM analysis of PS-BMSAC (a), RH-BMSAC (b), WC-BMSAC (c), and CS-BMSAC (d). The analysis indicated that the magnetic particles were embedded in the surface and internal channels of carbon materials. The catalyst consisted of a number of irregular shaped amorphous carbon particles, which were similar to that shown in previous literature (Goel *et al.* 2010). The only difference was observed in the load quantity and load degree of the magnetic particles. The magnetic particles were successfully loaded onto the surface and internal channels of carbon-based materials as indicated in Figs. 8a and 8d. The magnetic particles in the structure of CS-BMSAC (8d) was more loaded and had a more uniform distribution. However, magnetic particles were hard to find in Fig. 8c and in Fig. 8b. This suggested that the performance of RH- and WC-BMSAC would not be ideal.

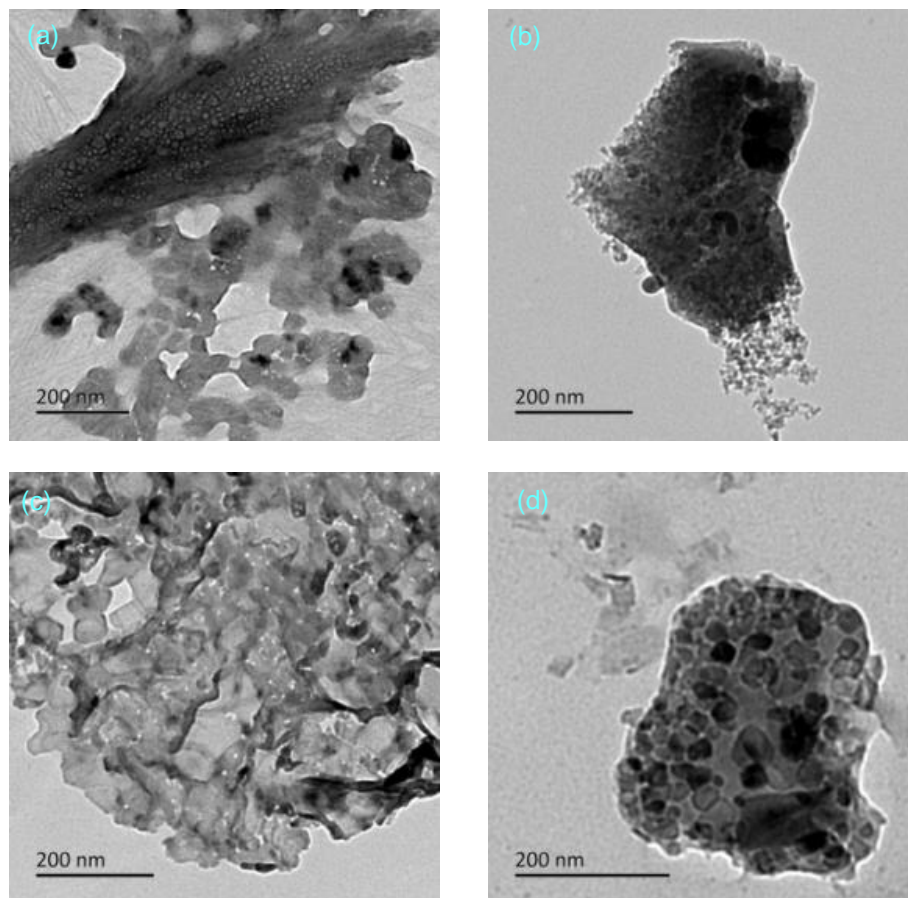


Fig. 8. TEM spectra of different carbon-based magnetic solid acid catalysts

SEM Analysis

Figure 9 shows the SEM micrographs of RH- (f), PS- (g), WC- (h), and CS- (k) BMSACs. It was clear from the SEM analysis that only the surface of CS-BMSAC (k) combined a large number of magnetic particles. Compared with previous literature (Shen *et al.* 2007), it was clear that the magnetic Fe_3O_4 particles were distributed in the carbon layer of the four catalysts.

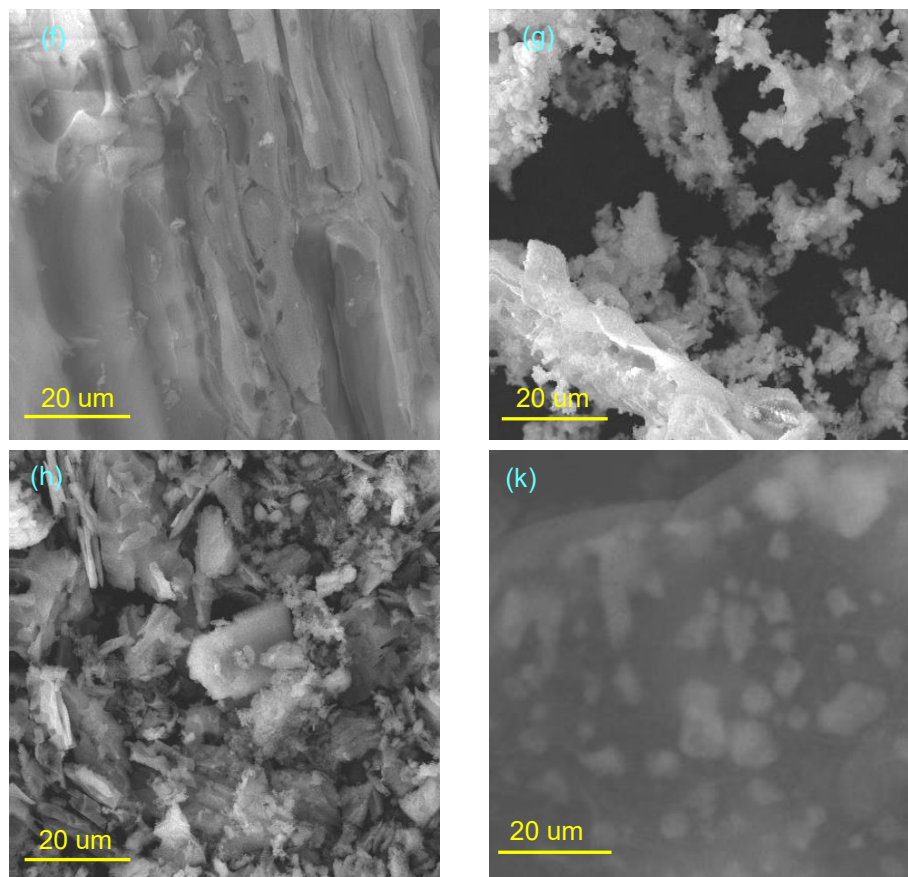


Fig. 9. SEM spectra of different carbon-based magnetic solid acid catalysts

Specific Surface Area Measurement

Based on the performance analysis of various CBMSACs, the performance of CS-BMSAC seemed the best. Therefore, the specific surface area of CS-BMSAC was analyzed. Table 4 and Fig. 10 show that the specific surface area of the catalyst was approximately 755 m²/g. As reported in previous literature (Garlapati *et al.* 2013), when the specific surface area of catalyst is larger, it will provide more active sites to increase the contact area of reactive group and cellulose molecules, which improves the catalytic activity of the catalyst.

Table 4. BET Analysis of Corn Straw-based Magnetic Solid Acid Catalyst

| P/P0 | Actual Adsorption Capacity (mL/g) | (P/P0)/(V*(1-P/P0)) | Single Point BET (m ² /g) | BET Surface Area (m ² /g) |
|-------|-----------------------------------|--|--------------------------------------|--------------------------------------|
| 0.21 | 2.19 | 0.12 | 758.70 | 755 |
| 0.19 | 2.13 | 0.11 | 748.60 | |
| 0.15 | 2.06 | 0.09 | 757.77 | |
| Slope | Intercept | Monolayer saturated adsorption capacity (mL) | Adsorption constant | Linear fitting degree |
| 0.55 | 0.005 | 1.80 | 109.16 | 0.99 |

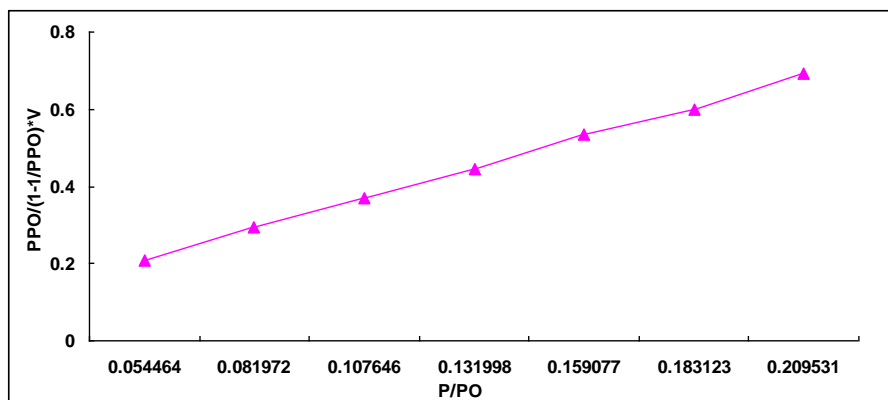


Fig. 10. Specific surface area of catalysis

Density of the Reactive -SO₃H Group

Since the H⁺ in the catalyst came from -SO₃H, the content of -SO₃H in all the catalyst was calculated according to the acid density. This was determined by potentiometric titration, and the results are shown in Fig. 11. It was seen that the content of the sulfonic acid group was different in the four kinds of catalysts. The sulfonic group density of CS-BMSAC was 2.5 mmol·g⁻¹ followed by that of PS-BMSAC, and the sulfonic group density of WC-BMSAC was the lowest. During the biomass carbonization-sulfonation process, the reaction followed a reversible electrophilic substitution pathway. However, because the alkyl side chain of biomass was an electron donating group, it increased the electron cloud density of the carbon carrier, which was advantageous to the adhesion of the -SO₃H group in the sulfonation reaction. As the CS contained more alkyl side chains, a large number of -SO₃H groups were attached on the carbon carrier, thereby the densities of -SO₃H group increased.

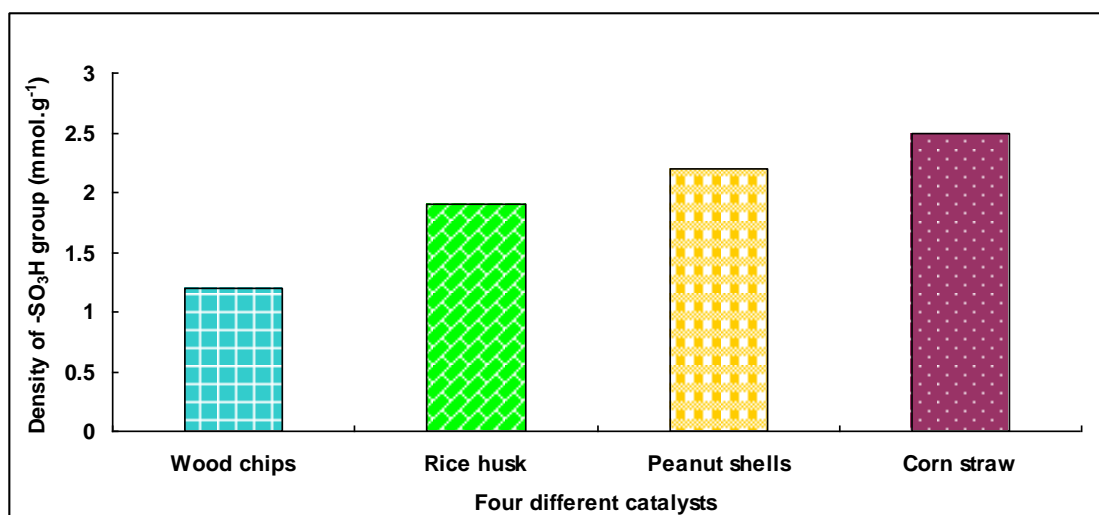


Fig. 11. Density of sulfonic acid group

CONCLUSIONS

1. A maximum reducing sugar yield of 58.8% was obtained from the hydrolysis of cellulose when CS-BMSAC was used. Compared to the traditional catalysts, there was approximately 5% increase of catalytic efficiency. The catalyst was recycled many times *via* a re-sulfonation method that enabled the regeneration activity.
2. The XRD analysis showed that the catalyst consisted of a random combination of amorphous carbon particles. The polymerization degrees of CS- and PS-BMSACs were higher and their structure was more stable. The SEM/TEM analysis revealed that in the CS-BMSAC, a number of magnetic particles were embedded on its surface and internal channels in a random way.
3. The BET analysis confirmed the large specific surface area (755 m²/g) of CS-BMSAC. This improved the catalyst dispersion and ensured good contact with the catalyst's active site and cellulose molecules.
4. Through the performance analysis of four kinds of CBMSACs, it was found that the CS-BMSACs indicated high catalytic activity and recycling rate, and its separation and recovery were easy. The performance of peanut shell-based magnetic solid acid catalyst ranked second. Thus, this study provided the basis for the effective utilization of biomass resources.

ACKNOWLEDGEMENTS

The authors are grateful for the support from the National Natural Fund Project: Mechanism study of cellulose hydrolysis by magnetic mimetic enzyme solid acid catalyst in water phase - 21376241; the support from the Introducing Foreign Advanced Forestry Technology, "948" Project: Import of corn straw biomass directional liquefaction technology - 2014-4-28; Henan Province Science and Technology Research Projects: The key technologies of using biomass to prepare levulinic acid esters fuel consumption and environmental benefits - 172102410030; The basic scientific research project funds of Henan Academy of Sciences: Study on the life cycle of corn stalk base acetyl propionate; High-end Scientific Research Platform of Jilin Province Department of Education: Jilin Province Comprehensive Utilization of Straw Technology Innovation Platform - [2014]C-1; Jilin Provincial Science and Technology Department patent promotion project: The construction of patent system for Forest Chemical Industry team (20170312028ZG); and Jilin Province Department of Education Science and Technology Research Project: Research on the degreasing technology of larch with high temperature and high pressure (2015172).

REFERENCES CITED

- Berry, C. C., and Curtis, A. S. G. (2003). "Functionalisation of magnetic nanoparticles for applications in biomedicine," *Journal of Physics D: Applied Physics* 36(13), 198-206. DOI: 10.1088/0022-3727/42/22/224003

- Chang, Z., Guo, C. X., Li, F., Duan, X., and Zhang, M., L. (2002). "Preparation and characterization of the novel magnetic nano-size solid acid catalyst," *Acta Chimica Sinica* 60(2), 298-304. DOI: 10.3321/j.issn:0567-7351.2002.02.019
- Chu, C. Y., Wu, S. Y., Tsai, C. Y., and Lin, C. Y. (2011). "Kinetics of cotton cellulose hydrolysis using concentrated acid and fermentative hydrogen production from hydrolysate," *International Journal of Hydrogen Energy* 36(14), 8743-8750. DOI: 10.1016/j.ijhydene.2010.07.072
- Chen, H., Wang, Y., Xu, G., and Yoshikawa, K. (2012). "Fuel-N evolution during the pyrolysis of industrial biomass wastes with high nitrogen content," *Energies* 5(12), 5418-5438. DOI: 10.3390/en5125418
- Du, F. Y., Zhang, X. Y., and Wang, H. X. (2004). "Studies on quantitative assay and degradation law of lignocellulose," *Biotechnology* 14(5), 46-48. DOI: 10.3969/j.issn.1004-311X.2004.05.024
- Garlapati, V. K., Kant, R., Kumari, A., Mahapatra, P., Das, P., and Banerjee, R. (2013). "Lipase mediated transesterification of *simarouba glauca*, oil: A new feedstock for biodiesel production," *Sustainable Chemical Processes* 1(1), 1-6. DOI: 10.1186/2043-7129-1-11
- Goel, S., Mazumdar, N. A., and Gupta, A. (2010). "Synthesis and characterization of polypyrrole nanofibers with different dopants," *Polymers for Advanced Technologies* 21(3), 205-210. DOI: 10.1002/pat.1417
- Keiluweit, M., Nico, P. S., Johnson, M. G., and Kleber, M. (2010). "Dynamic molecular structure of plant biomass-derived black carbon (biochar)," *Environmental Science and Technology* 44(4), 1247-1253. DOI: 10.1021/es9031419
- Ke, F., Qiu, L. G., and Zhu, J. (2013). "Fe₃O₄@MOF core-shell magnetic microspheres as excellent catalysts for the Claisen-Schmidt condensation reaction," *Nanoscale* 6(3), 1596-1601. DOI: 10.1039/c3nr05051c
- Nunes, L. J. R., Matias, J. C. O., and Catalão, J. P. S. (2016). "Biomass combustion systems: A review on the physical and chemical properties of the ashes," *Renewable & Sustainable Energy Reviews* 53(15), 235-242. DOI: 10.1016/j.rser.2015.08.053
- Sathishkumar, P., Arulkumar, M., and Palvannan, T. (2012). "Utilization of agro-industrial waste *Jatropha curcas*, pods as an activated carbon for the adsorption of reactive dye Remazol Brilliant Blue R (RBBR)," *Journal of Cleaner Production* 22(1), 67-75. DOI: 10.1016/j.jclepro.2011.09.017
- Shen, B., Li, Y., Wang, Z. F., and He, N. Y. (2007). "Catalytic activity of palladium supported on magnetic nanoparticles for Heck reaction," *Chinese Journal of Catalysis* 28(6), 509-513. DOI: 10.3321/j.issn:0253-9837.2007.06.007
- Sinirlioglu, D., Aslan, A., Muftuoglu, A. E., and Bozkurt, A. (2014). "Synthesis and proton conductivity studies of methacrylate/methacrylamide-based azole functional novel polymer electrolytes," *Journal of Applied Polymer Science* 131(4), 1001-1007. DOI: 10.1002/app.39915
- White, R. J., Budarin, V., Luque, R., Clark, J. H., and Macquarrie, D. J. (2009). "Tunable porous carbonaceous materials from renewable resources," *Chemical Society Reviews* 38(12), 3401-3418. DOI: 10.1002/chin.201014216
- Wu, R. N., Wang, T. H., Xiu, Z. L., Guo, F., Pan, Y. Q., and Yin, J. Z. (2009). "Preparation of a biomass carbon-based solid acid catalyst," *Chinese Journal of Catalysis* 30(12), 1203-1208. DOI: 10.3321/j.issn:0253-9837.2009.12.004
- Yu, D. L., Zhang, Y. F., and Li, X. Y. (2013). "Study on preparation of magnetic carbon-

- based solid sulfoacid catalyst and its catalytic properties,” *Chemistry and Bioengineering* 30(10), 34-37. DOI: 10.3969/j.issn.1672-5425.2013.10.009
- Zhang, Z. B., Lu, Q., Ye, X. N., Li, W. T., Hu, B., and Dong, C. Q. (2015). “Production of phenolic-rich bio-oil from catalytic fast pyrolysis of biomass using magnetic solid base catalyst,” *Energy Conversion and Management* 10(106), 1309-1317. DOI: 10.1016/j.enconman.2015.10.063
- Zhou, W., Yoshino, M., Kita, H., and Okamoto, K. (2001). “Carbon molecular sieve membranes derived from phenolic resin with a pendant sulfonic acid group,” *Industrial & Engineering Chemistry Research* 40(22), 4801-4807. DOI: 10.1021/ie010402v

Article submitted: April 16, 2017; Peer review completed: August 12, 2017; Revised version received: August 19, 2017; Accepted: August 20, 2017; Published: August 28, 2017.

DOI: 10.15376/biores.12.4.7525-7538